A Bulky Glycocalyx Fosters Metastasis Formation by Promoting G1 Cell Cycle Progression

Elliot C. Woods[1], J. Matthew Barnes[2], Michael W. Pickup[2], Kayvon Pedram[1], FuiBoon Kai[2], Michael J. Hollander[1], Valerie M. Weaver[2,3], Carolyn R. Bertozzi[1,4]

[1] Department of Chemistry, Stanford University, California, USA

[2] Center for Bioengineering and Tissue Regeneration, Department of Surgery, University of California, San Francisco, California, USA

[3]Departments of Anatomy, Bioengineering and Therapeutic Sciences, and Radiation Oncology, Eli and Edythe Broad Center of Regeneration Medicine and Stem Cell Research, and UCSF Helen Diller Comprehensive Cancer Center, UCSF, San Francisco, California, USA

[4] Howard Hughes Medical Institute, Stanford University, California, USA

Abstract

Metastasis depends upon cancer cell growth and survival within the metastatic niche. Tumors which remodel their glycocalyces, by overexpressing bulky glycoproteins like mucins, exhibit a higher predisposition to metastasize, but the role of mucins in oncogenesis remains poorly understood. Here we report that a bulky glycocalyx promotes the expansion of disseminated tumor cells *in vivo* by fostering integrin adhesion assembly to permit G1 cell cycle progression. We engineered tumor cells to display glycocalyces of various thicknesses by coating them with synthetic mucin-mimetic glycopolymers. Cells adorned with longer glycopolymers showed increased metastatic potential, enhanced cell cycle progression, and greater levels of integrin-FAK mechanosignaling and Akt signaling in a syngeneic mouse model of metastasis. These effects were mirrored by expression of the ectodomain of cancer-associated mucin MUC1. These findings

functionally link mucinous proteins with tumor aggression, and offer a new view of the cancer glycocalyx as a major driver of disease progression.

Manuscript

Introduction

Cell surface mucins, such as MUC1 and MUC16, are so consistently upregulated in epithelial cancers that they are considered reliable biomarkers of the disease.(1)(2) Despite their importance for diagnosis and prognosis, the mechanisms by which mucins might promote malignancy remain largely speculative.(3) To date, the majority of studies exploring the role of mucins in determining tumor phenotype have focused on the signaling function of these molecules, which resides within their short cytoplasmic tail. Yet, a striking and defining feature of cell surface mucins is their long, densely glycosylated ectodomain, which can extend hundreds of nanometers from the plasma membrane.(4) Consequently, mucins can profoundly enhance the bulk physical properties of the glycocalyx, which is a composite of the polysaccharides and glycoproteins that project from the plasma membrane and decorate all cells.

We recently showed that the bulk physical properties of the glycocalyx can exert profound effects on cellular behavior. These effects include a reorganization of cell surface receptors such as integrins. This reorganization alters their activation state and influences not only their ability to interact with extracellular matrix (ECM) ligands but also their synergistic downstream signaling with growth factor receptors.(5,6) By occluding the majority of binding sites, an expansive glycocalyx paradoxically promotes integrin clustering by creating a kinetic funnel in which integrins are most likely to bind

to the ECM where bonds are already formed.(7) In this regard, in vitro studies revealed that increasing the bulkiness of the glycocalyx enhanced the ability of nonmalignant mammary epithelial cells to grow and survive under minimally adhesive conditions whereas otherwise the cells underwent anoikis.(5,8,9) Whether a bulky glycocalyx similarly modulates cell growth and survival *in vivo,* however, has yet to be unambiguously tested.

Importantly, we and others have also noted that tumor aggression is frequently associated with an increased expression of mucins which enhance the bulkiness of the glycocalyx and, similarly, that circulating epithelial tumor cells typically express an abundance of mucins.(5) Concomitantly, primary tumor xenografts that overexpress MUC1 grow and metastasize more aggressively (10) and mice deficient in MUC1 resist formation of spontaneous tumors (11). Together, these observations raise the intriguing possibility that tumor associated mucin expression may foster tumor progression and aggression by enhancing either tumor cell growth and survival or both by modulating integrin and growth factor receptor signaling.

Herein, we report that increasing the thickness of the glycocalyx promotes tumor metastasis by permitting cell cycle progression to facilitate cell proliferation at the metastatic site. We modulated glycocalyx thickness both genetically through ectopic expression of a tailless (signaling defective) MUC1 and more definitively by coating cells with synthetic glycopolymers with long-term cell surface retention that were designed to emulate the structure of mucin ectodomains (Fig. 1A).(8) The longevity of the synthetic glycopolymers was facilitated by developing the chemistry so that the tail terminated in a cholesterylamine lipid at one end, which effectively drives spontaneous insertion into cell

membranes based on mass action and the hydrophobic effect. We previously found that this particular lipid confers a long cell surface residence time to glycopolymer conjugates by mediating continuous recycling from an internal reservoir.(8) The core of the glycopolymer comprises *N*-acetylgalactosamine (GalNAc) residues affixed to a poly (methyl vinyl ketone (MVK)) backbone via oxime linkages. The spacing afforded by this structure approximates that of GalNAc-α-Ser/Thr clusters within native mucins. Likewise, GalNAc-modified poly (MVK) glycopolymers emulate the physical characteristics of native mucins such as length and stiffness.(5) However, unlike the more complex glycans found in native mucins, which can engage in biochemical interactions,(12) the GalNAc residues we used here are considered biochemically inert in mammalian systems. Thus, these synthetic structures allowed us to model mucins' biophysical contribution to the glycocalyx without any confounding contributions from their cytosolic or extracellular biochemical activity. As well, the living polymerization chemistry used to generate the glycodomains enabled precise control of polymer length with high homogeneity.(13) Living polymerization techniques allow for the synthesis of polymers of very homogeneous lengths, a necessity for the comparison of the effects of long and short polymers. In this work, we used short glycopolymers of ~3 nm in length (degree of polymerization (DP) = 36 monomer units) and long glycopolymers that were ~ 90 nm in length (DP = 719 monomer units). As a point of comparison, integrin heterodimer pairs extend roughly 20 nm from the cell membrane (Fig. 1A).(14)

Results

Metastasis is a multistep process that requires cancer cells to overcome many checks to their irregular growth – limited not only by ability to disseminate but also to survive and thereafter to grow and expand at the metastatic site. The nonmalignant mammary epithelial cell line, MCF-10A, offers a unique model for oncogenic progression.(15) These cells, though immortal, lack the ability to grow or survive efficiently in a soft matrix, and therefore serve as an ideal cell line to evaluate the effects of the glycocalyx on mammary epithelial cell behavior in the context of a metastatic site.(16) Our prior studies suggested that a bulky glycocalyx permitted not only the survival but also the growth of these mammary epithelial cells in an *in vitro* model of a minimally adhesive microenvironment. Thus, we asked whether a bulky glycocalyx would permit both the survival and the growth and expansion of disseminated mammary epithelial cells *in vivo*. MCF-10A cells were painted with our glycopolymers, then injected into the venous system of nude mice, where they accumulated in the lungs regardless of glycopolymer length. We found that those cells treated with long glycopolymer mucin-mimetics survived longer, as demonstrated by delayed activation of the apoptosis marker cleaved caspase-3 (CC3), than those decorated with short glycopolymers (Figure 1—figure supplement 1), consistent with our *in vitro* studies. Nevertheless, the cells eventually died and therefore ultimately failed to form metastatic lesions, leaving us unable to determine the potential effect of the glycocalyx on proliferation. Thus, to unambiguously address whether or not a bulky glycocalyx might influence tumor behavior and metastasis by regulating cell proliferation, independent of cell survival, we assessed the influence of the glycopolymers on the growth and

metastatic efficiency of the dormant-prone tumor cell line from the syngeneic 4TO7/Balbc model.

The murine cell line 4TO7 is a Balb/c syngeneic mammary carcinoma that is able to efficiently disseminate and survive for prolonged periods of time at metastatic sites such as the lung.(17) However, the tumor cells in this model form predominately dormant tumors because they are unable to proliferate efficiently at the target site. These 4TO7 cells, therefore, provided us the ideal model to specifically address the contribution of a bulky glycocalyx on cell proliferation and G1 cell cycle transit *in vivo*.

The glycocalyx increases metastatic potential in a size dependent manner

We first confirmed that the mucin-mimetic glycopolymers were long-lived on 4TO7 cell surfaces in culture, as previously found with other cell lines (Fig. 1B).(8) Next, we grew mCherry-luciferase fusion-transfected 4TO7 cells to subconfluency, painted them with glycopolymers, then injected them into the tail veins of Balb/c mice (Fig. 1C). Veins lead directly to the right heart where cells next meet the capillary beds of the lungs and are lodged. Every 4-5 days mice were anesthetized and given an intraperitoneal (IP) injection of luciferin for bioluminescence imaging (BLI) (Fig. 1D). By day 13, mice injected with 4TO7 cells coated with long glycopolymers were generating greater photon flux, on average, than their counterparts injected with short glycopolymer-treated cells, suggesting a higher density of luciferase-expressing cells and thus an increased tumor burden (Figs. 1D and 1—figure supplement 1). In particular, we noted that the increase in BLI over time in the long glycopolymer group appeared to approximate an exponential growth-type trend, while the short group did not (Fig. 1—figure supplement 2).

Importantly, we measured no significant difference in accumulation of tumor cells in the lungs between treatment groups as measured by BLI at Day 0.

On day 15, the mice were sacrificed and necropsies were performed. We observed gross differences in tumor burden between glycopolymer treatment groups (compare Figures 1E and 1F). Lungs were weighed wet then fixed in 4% paraformaldehyde and embedded in paraffin wax for whole histological sectioning. Hematoxylin and eosin (H&E) staining revealed qualitative differences in tumor burden, and immunohistochemistry (IHC) staining for mCherry confirmed that tumors were derived from exogenous mCherry-luciferase transfected 4TO7 cells and did not arise *de novo* (Figs. 1G and 1H).

Lung tissue is spongy and consists of an abundance of negative space that can be filled with air during respiration. Tumors, by comparison, are dense and contain relatively little negative space. Consequently, in a vein-to-lung model of metastasis, lung mass can be a strong indicator of tumor burden. We found that the lungs of mice injected with 4TO7 cells endowed with a bulky glycocalyx were significantly heavier than lungs from mice injected with short glycopolymer-bearing cells (Fig. 1I). In addition to mass, we directly quantitated the number of mets per lung. For each mouse, we counted every met in the whole lung H&E section taken 5 millimeters (mm) into sectioning. Long glycopolymer-treated 4TO7 cells produced, on average, more than twice the number of mets per mouse when compared to short (Fig. 1J). Thus, merely increasing the thickness of the glycocalyx was sufficient to increase the metastatic potential of otherwise poorly metastasizing murine carcinoma cells. Importantly, the short glycopolymers did not increase the metastatic potential of 4TO7 cells when compared to mock (PBS) treated

cells (Fig. 1—fig. supplement 3). Metastasis is an inefficient process—few circulating tumor cells actually give rise to metastatic tumors—and the prevailing view is that survival and proliferation at the secondary site is rate limiting.(18) Therefore, we wondered if this increased metastatic potential could be due to increased growth, survival, or both.

Quantitative immunofluorescence (IF) imaging of phosphorylated histone H3 (pH3)—a marker of mitosis—and cleaved caspase-3 (CC3)—a marker of apoptosis—revealed that mets from long glycopolymer-treated cells had higher rates of proliferation than those from cells treated with short glycopolymers (Figs. 1K and 1L). But, the rates of apoptosis were similar (Figs. 1K and 1M). While surprising at first, given our knowledge that a thick glycocalyx improves survival in minimal adhesion settings, we reasoned that by day 15 the survival phenotype had likely run its course—cells unable to survive in that niche may have died days earlier. These data corroborated our BLI results and indicated that the glycocalyx likely affects metastatic proliferative competency *in vivo*.

A thick glycocalyx drives cell cycle progression via the PI3K-Akt axis

To gain mechanistic insight into this apparent proliferative effect, we tested the effects of modulating glycocalyx thickness on cell growth in a soft matrix *in vitro* model. We used fibronectin-functionalized polyacrylamide (PA) gels whose stiffness can be controlled by varying both acrylamide concentration and crosslinking frequency.(19) We painted MCF-10A cells with short or long mucin-mimetic glycopolymers, or with vehicle (PBS), then plated them at low density on fibronectin-functionalized soft PA gels

(Young's modulus = 400 Pa) so that nearly all cells were isolated, minimizing cell-cell interactions. After 72 hours, we imaged the gels and quantified the number of cells in each observed colony. The long glycopolymer-painted cells formed colonies with, on average, twice as many cells as colonies formed by the short glycopolymer-treated cells or PBS-treated controls (Figs. 2A-C). And the percentage of colonies growing beyond two cells nearly tripled for long-glycopolymer-treated cells verses PBS-treated controls, indicating that this increase in mean colony size was not due merely to a few large colonies (Fig. 2D).

To test that this phenotype required cell-surface residence of the long glycopolymers, we compared the effects of the cholesterylamine-anchored molecules, which persist on the plasma membrane for several days even after cell division, with those of a phospholipid-functionalized glycopolymer that is lost from the cell surface within several hours.(8) Cells treated with these short-lived but equally long glycopolymers did not produce larger colonies compared to PBS treatment alone (Fig. 2—figure supplement 1). Thus, the effects measured in Figs. 2C and 2D are likely mediated by glycopolymers resident on the cell surface.

To further test our hypothesis that a bulky glycocalyx permits proliferation in the metastatic niche, we analyzed markers of cell cycle progression. Cells were painted with short or long glycopolymers, or with vehicle (PBS), then plated on either soft (Young's modulus = 400 Pa) or stiff (Young's modulus = 60,000 Pa) fibronectin-functionalized PA gels, the latter being a positive control for integrin activation.(20) After allowing them to adhere for 6 hours, cells were lysed and the lysates analyzed by immunoblotting. We found that cells plated on stiff PA gels, which offer a rich adhesion setting, produced

higher levels of cyclin D (a protein required for cell cycle progression) and showed higher levels of pH3 than those on adhesion-poor soft gels (Fig. 2E and Fig. 2—fig. supplement 2A). Long glycopolymer-treated cells also demonstrated increased cyclin D and pH3 levels, compared to short glycopolymer- and PBS-treated cells, even on soft gels, suggesting that a thick glycocalyx drove proliferation and cell cycle progression in this poor adhesion setting.

Integrin activation and growth factor signaling form, in logic terms, an "AND gate" for cell cycle progression in nontransformed cells.(21) We sought to determine whether a bulky glycocalyx alters this fundamental control mechanism. After serum-starving MCF-10A cells for 72 hours, we lifted them, painted them with long or short glycopolymers, or with vehicle. The cells were plated on gels as in Figure 2E, except now in serum-free media, and then lysed after 6 hours. A lack of growth factor signaling reduced cyclin D1 and pH3 levels to below the detection limit, even when cells were grown on stiff gels or endowed with a bulky glycocalyx (Fig. 2F). The underlying drivers of proliferation therefore, including growth factor signaling requirements, appeared to be unaltered by glycocalyx thickness in this model.

To discern the factors responsible for increased cell cycle progression of cells with thicker glycocalyces, we examined Erk and Akt, the mitogen activated protein kinases (MAPKs) thought to be central to adhesion-mediated control of cell cycle progression.(22) After serum starvation for 72 hours, cells were coated with glycopolymers or vehicle, and plated on PA gels in serum-free media for 6 hours. The cells were then challenged with epidermal growth factor (EGF) for 15 minutes and then lysed. A bulky glycocalyx increased Akt phosphorylation, a proxy for activation, on soft

gels to a level that was comparable to that observed from cells on stiff gels (Fig. 2G and Fig. 2—fig. supplement 2B). As well, IF analysis of tissue sections from the experiments in Figure 1 revealed an increased Akt activation, as measured by staining for phosphorylated Akt substrate, *in vivo* for long-glycopolymer bearing tumor cells (Fig. 2—fig. supplement 3). Erk phosphorylation, however, remained unchanged (Fig. 2G). Consistent with this finding, we repeated the colony formation experiments and found that proliferation of long glycopolymer-painted cells was blocked by an inhibitor of phosphoinositol-3 kinase (PI3K), an upstream activator of Akt (Fig. 2H) and an inhibitor of MEK—a kinase downstream of PI3K (Fig. 2—fig. supplement 4). A bulky glycocalyx, therefore, drives cell cycle progression via the PI3K-Akt axis.

We confirmed the role of cell cycle progression in promoting metastasis *in vivo* by IF staining of the lung mets from the experiments in Figure 1. Mets in lungs from mice injected with cells bearing long glycopolymers expressed significantly more of the cell cycle progression marker cyclin D1 than those formed from cells expressing short glycopolymers (Figs. 2I and 2J).

A thick glycocalyx stimulates integrin-FAK mechanosignaling

Next, we sought to test our hypothesis that this phenotype is driven by integrin-focal adhesion kinase (FAK) signaling. FAK disseminates adhesion information from focal adhesions to the rest of the cell via autophosphorylation at tyrosine 397, as well as increased phosphorylation at tyrosine 925, presumably through Src kinase activation.(23) Western blotting with phospho-specific antibodies revealed that possession of a thick glycocalyx led to enhanced activation of FAK (Fig. 3A and Fig. 3—fig. supplement 1).

These effects on FAK were mirrored by adhesion of untreated cells to a stiff matrix. By contrast, cells coated with short glycopolymers, or untreated cells, plated on a soft matrix showed comparatively less phosphorylation on FAK. Reciprocally, cells treated with long glycopolymers along with a nonlethal dose of a specific inhibitor of FAK were unable to form colonies on soft matrices, whereas vehicle (DMSO)-treated, long glycopolymer-coated cells retained colony forming activity (Fig. 3B).

To determine whether enhancement of adhesion signaling due to a bulky glycocalyx also occurs *in vivo*, we probed FAK phosphorylation status in the mets from Figure 1. Long glycopolymer-treated cells formed tumors with significantly more FAK activation than tumors formed from short glycopolymer-bearing cells (Figs. 3C and D). These data, taken with the results in Figure 2, support a model for glycocalyx-dependent enhancement of proliferation in minimal-adhesion settings. A bulky glycocalyx drives integrin clustering through kinetic funneling, leading to increased signaling from focal adhesion-associated proteins such as FAK. In combination with growth factor signaling, this leads to enhanced MAPK activation, such as Akt phosphorylation, which then promotes G1 cell cycle progression through expression of proteins like the cyclins (Fig. 3E).

The MUC1 ectodomain is sufficient to increase the metastatic potential of 4TO7 cancer cells

Lastly, for physiological relevance, we evaluated the effects of a natural mucin ectodomain on the metastatic potential of 4TO7 cells. We utilized a cytoplasmic truncation of MUC1 (MUC1ΔCT), the mucin most commonly overexpressed in breast

and ovarian cancers, to limit any cytoplasmic signaling which might confound our results. We transfected mCherry-luciferase expressing 4TO7 cells with MUC1ΔCT under the control of a doxycycline (dox)-inducible promoter. We grew these cells to subconfluence, treated them with doxycycline (200 ng/ml) or vehicle (PBS) for 24 hours, then lifted them and immediately injected them into Balb/c mouse tail veins (Fig. 4A). As previously, mice were monitored every 4-5 days via BLI measurements and sacrificed on day 15.

BLI photon flux revealed that MUC1ΔCT-expressing cells formed mets that were growing more rapidly than those formed from MUC1ΔCT-negative cells (Fig. 4—figure supplement 1). Whole lung sectioning, H&E staining and IHC on mCherry revealed a dramatic qualitative difference in tumor burden (Figs. 4B and 4C). Wet lung mass was nearly doubled in mice injected with MUC1ΔCT-expressing cells versus control (Fig. 4D). Nearly three times the number of mets were formed in the lungs of mice injected with cells expressing the mucin ectodomain compared to those that were not (Fig. 4E). pH3 IF staining revealed that more than twice the number of nuclei in MUC1ΔCT-expressing cells were actively mitotic. And while the values did not reach statistical significance ($p = 0.06$), CC3 levels were trending towards lower values in MUC1ΔCT-expressing mets (Figs. 4F-H). Staining for pY397-FAK, cyclin D1 and pAkt substrate demonstrated that the MUC1 ectodomain increases mechanosignaling, cell cycle progression and MAPK activity in lung mets, further supporting our model (Figs. 4I-K and Fig. 4—fig. supplement 2). These results dramatically demonstrate the effect that the mucin ectodomain can have on metastatic cells *in vivo*.

Discussion

Mucin overexpression is commonly observed in epithelial cancers. MUC1 in particular is overexpressed in ~64% of tumors of all types diagnosed each year in the U.S. (24), rendering MUC1 one of the most prominently dysregulated genes in cancer. As a point of reference, Ras (*K*-, *H*- and *N-RAS* combined) mutations are estimated to occur in 9-30% of all cancers.(25) Hypotheses regarding the mechanism by which MUC1 overexpression drives cancer progression have focused almost entirely on biochemical interactions of its 72-residue cytosolic domain (24), which represents <10% of the overall protein sequence. The bulk of MUC1 resides outside the cell where it dominates the physical properties of the glycocalyx. In previous work, we showed that this ectodomain profoundly influences focal adhesion formation, integrin signaling, and survival in a minimal adhesion setting.(5) But this effect alone cannot explain the striking effect of MUC1 ectodomain expression on metastatic burden that we observed in this study (Fig. 4). Our data herein show that a bulky glycocalyx, achieved either with synthetic or natural mucins, also promotes proliferation in the metastatic niche. The mucin ectodomain promotes mechanosignaling and enhances cell cycle progression via the PI3K-Akt axis. This model unifies the structure of mucins with their consistent overexpression in metastatic disease (26) and the correlation of their overexpression with poor prognosis.(2,27–29) As well, importantly, our results imply that drugs targeting the cytoplasmic tail of MUC1 will be missing a key pathophysiologic mechanism.

It should be noted that in addition to their physical influence, the glycans on mucins have been found to participate in biochemical interactions. For example, sialylated mucin-associated glycans engage the Siglec family of immunomodulatory

receptors and may therefore tune the response of critical effector cells in the tumor microenvironment.(30–32) Thus, mucins' influence on cancer likely reflects many functional modalities, each contributing differentially to various facets of disease progression. From this vantage point, mucins are prime targets for therapeutic intervention and warrant increased focus on avenues for their disruption.

Acknowledgements

The authors would like to thank Dr. Jon Lakins for the rtTA lentiviral vector. We would also like to thank Drs. Ori Maller, Dwight Chambers, and Brian Belardi for helpful discussions. This work was funded by a grant from the US National Institutes of Health (R01GM59907). ECW was supported by a predoctoral fellowship (F31CA200544).

Materials and Methods

Mucin-mimetic glycopolymers

Glycopolymers were synthesized as previously described (8). Briefly, lipid-conjugated RAFT agents were synthesized, from which methyl vinyl ketone was polymerized, to generate polymers of various lengths with low polydispersities. The ketone pendant groups were functionalized with alkoxy-amine containing *N*-acetylgalactosamine monomers and purified to give the final lipid-terminated glycopolymers.

Cell culture

MCF-10As were acquired from ATCC (CLR-10317), met the published morphological characteristics described on ATCC, used within 30 passages, confirmed to be

mycoplasma free, and maintained in recommended media: DMEM/F12 without phenol red, supplemented to contain 5% horse serum (Invitrogen), EGF (20 ng/ml from Peprotech), hydrocortisone (0.5 mg/ml from Sigma), cholera toxin (100 ng/ml from Sigma), insulin (10 ¥ g/ml from Sigma) and 1% penicillin/streptomycin.

4TO7 cells were a kind gift from Dr. Philip Owens (Vanderbilt University), met the morphologic characteristics described on ATCC, used within 30 passages, confirmed to be mycoplasma free and were maintained in DMEM with 10% FBS and 1% penicillin/streptomycin.

Glycopolymer loading onto cell surfaces

Lipid-anchored glycopolymers spontaneously insert into cell membranes due to the hydrophobic effect and mass action. Where noted in experimental sections below, cells in suspension are mixed with stock concentrates of aqueous solutions of glycopolymers and allowed to be labeled for 1 hour at room temperature. The cells are then pelleted, the labeling solution aspirated, and the excess glycopolymers washed away by an additional dilution-pelleting step. Details of the synthesis and use of glycopolymers used in this study can be found in Woods *et al* (8).

Cell surface measurement of glycopolymers

Glycopolymers bearing a biotin molecule on the terminus opposite the lipid tail were incubated with cells. Cells were washed and incubated in warm complete media for the desired length of time, then washed with ice-cold PBS to reduce lipid trafficking and

incubated with fluorescent anti-biotin antibodies at 4 °C for 20 min, then washed and analyzed by flow cytometry. More details of this method of measuring recycling of lipid-born glycopolymers can be found in Woods *et al* (8).

mCherry-Luciferase transfection

4TO7 cells were stably transduced with an mCherry-luciferase fusion with lentivirus (pLV). Cells were selected with puromycin (1μg/mL) for purity then used as described (33).

MUC1ΔCT transfection

4TO7 cells were stably transduced with reverse tetracycline-controlled transactivator (rtTA, tet-on system) lentivirus (pLV-neo). After neomycin (100μg/mL) selection of rtTA-integration, cells were co-transfected (Lipofectamine 3000, Thermo Fisher, per manufacturer's recommendation) with a transposon (PiggyBac) expressing human MUC1ΔCT (cytoplasmic tail-deleted) and PiggyBac transposase. Cells were selected in puromycin (1μg/mL) for purity and then used as described (33).

Polyacrylamide cell substrates

Fibronectin-functionalized PA substrates were synthesized as described previously with a few modifications. Briefly, methacrylate-functionalized cover glass was used with dichlorodimethylsilane-functionalized cover glass to create a sandwich between which PA gels were allowed to polymerize. Gels were functionalized with the heterobifunctional molecule N6. Fibronectin then was conjugated to the gels via N6's

amine-coupling chemistry. Gels were rinsed and warmed with media before cells were added.

Colony formation experiments

MCF-10A cells were lifted with trypsin, counted, then incubated with 10 μM polymers in PBS or PBS alone at 10^7 cells per ml for 1 hour at room temperature. Cells were washed, then brought up into warm media and plated onto fibronectin-functionalized substrates. After 72 hours in culture, images were taken from 9 random fields of view each from two technical replicate gels per experimental condition, and the experiment was replicated in entirety thrice.

Western blots

MCF-10A cells were lifted and coated with polymers as in the colony experiments. Six hours after plating at 4.6 x 10^3 cells per cm^2, the cells were rinsed with ice-cold PBS, then lysed with M-PER lysis buffer (Thermo Fisher) containing phosphatase inhibitors and protease inhibitors. Lysates were subjected to SDS-PAGE and transferred to nitrocellulose membranes. Primary antibodies were from Cell Signaling Technology and used as recommended. HRP-conjugated secondary antibodies were from Cell Signaling Technology and used as recommended.

Mice

All mice were maintained in accordance with University of California Institutional Animal Care and Use Committee guidelines under protocol AN105326. Four week old

female Balb/c or nude mice were obtained from Jackson Labs and allowed to acclimate for 2 weeks before experiments were performed.

Tail vein metastasis model

Mice were restrained and tail vein injections were performed with 100 µl at 10^6 cells per ml. Mice were not fed doxycycline—Dox (+) cells were treated for 24 hours before injections with 200 ng/ml in complete media. For bioluminescence imaging, mice were injected i.p. with D-luciferin at 15mg/kg, anesthetized with 2.5% isofluorane and luciferin was allowed to circulate for 10 minutes prior to live animal imaging on an IVIS Spectum imaging system (PerkinElmer). Sample sizes were determined using a two-sample test, a power of 0.90, and a Type I error of 0.05 with data collected from pilot studies.

Histology

Paraffin-embedded lung tissues were sectioned, deparaffinized, and stained with hematoxylin and eosin before imaging.

Immunohistochemistry

Paraffin-embedded lung tissues were sectioned at 5 µm, deparaffinized, and rehydrated using graded ethanol washes. Sodium citrate buffer was used for antigen retrieval. Sections were blocked with BSA then incubated with primary antibodies overnight. Anti-mCherry antibodies were from Abcam and used as recommended. Biotinylated secondary antibodies were from Cell Signaling Technology and used as recommended. DAB

peroxidase substrate kit from Vector Labs was used as recommended. Sections were then dehydrated using graded ethanol washes and mounted in Permount (Sigma). Mounted sections were imaged by light microscopy.

Immunofluorescence

Paraffin-embedded lung tissues were sectioned at 5 μm, deparaffinized, and rehydrated using graded ethanol washes. Sodium citrate buffer was used for antigen retrieval. Sections were blocked with BSA then incubated with primary antibodies overnight. pH3 antibodies were from Cell Signaling Technology and used as recommended. Fluorescent secondary antibodies were from Jackson ImmunoResearch and used as recommended. Sections were wet-mounted then imaged by confocal microscopy.

Quantification of immunofluorescence

After microscopy, images were analyzed using ImageJ software. DAPI-stained nuclei were counted using the 'Analyze particles' tool. Signal from antibodies of interest was measured using the 'Measure' tool set to output 'mean' pixel intensity. Quotients were obtained by dividing either the number of positive nuclei (pH3) or mean pixel intensity (other antibodies) by the number of nuclei—thereby accounting for tumor density or size in our image analysis. Quotients were normalized to negative controls and plotted as normalized average signal per cell.

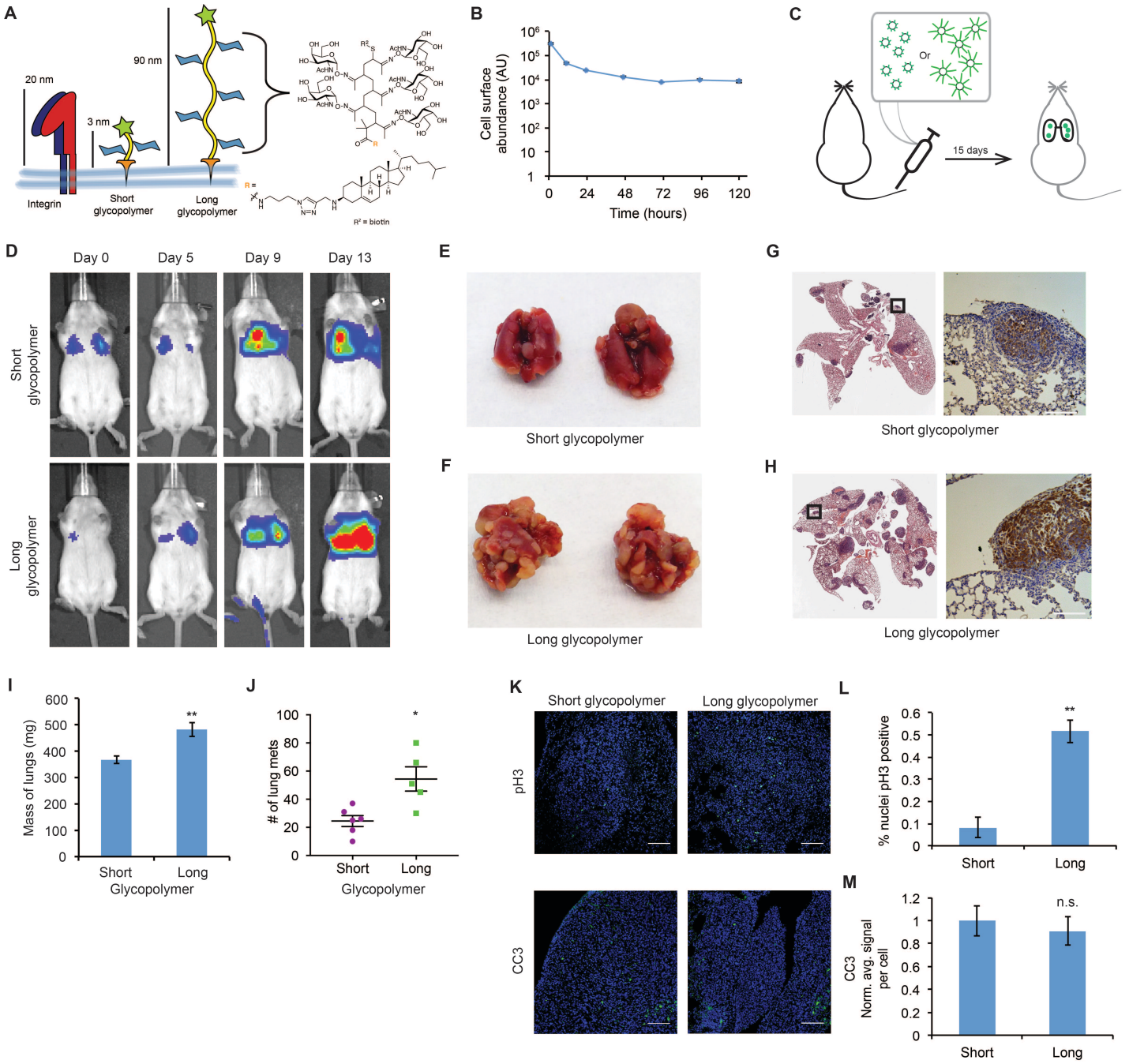

Figure 1: The glycocalyx increases metastatic potential in a size dependent manner

A) Mucin-mimetic glycopolymers consist of a poly(methyl vinyl ketone) polymer with pendant GalNAc residues. The glycopolymer terminates in a synthetic sterol for insertion into cell membranes. Precise synthetic control allows for glycopolymers to be made much larger or smaller than integrins. B) Glycopolymers reside on 4TO7 cell surfaces for days. C) Experimental scheme for Figure 1. Balb/c mice were injected with syngeneic 4TO7 mammary carcinoma cells bearing long or short glycopolymers. Tail vein injections lead cells to the capillary beds of the lungs where subsequent metastatic growth can be observed. D) Bioluminescence Imaging (BLI) of mice injected with either long or short glycopolymer-bearing cells. E) and F) Gross appearance of lungs excised from mice at 15 days

post injection. G) and H) H&E staining and IHC labeling for mCherry indicating presence of exogenously introduced cells. I) Lungs excised during necropsy were weighed, wet, before fixing. J) Frank mets were counted on whole lung sections at 5 mm into sectioning for each mouse and grouped according to glycopolymer treatment type of injected cells. K) IF staining of mets for the mitotic marker pH3 or apoptotic marker CC3 in green. DAPI nuclear staining is shown in blue. L) and M) Quantification of IF signal. For pH3, shown is the quotient of positive over total nuclei. For CC3, total signal was normalized to the average signal per nuceli in mets from short glycopolymer treated cells. For both L and M, shown is the mean ± SEM of three mice per group from which 3-4 tumors were averaged each. For I and J, shown is the mean ± SEM of n = 6 for mice injected with short glycopolymer-treated cells and n = 5 for mice injected with long glycopolymer-treated cells. Scale bars are 100 μm. *$p < 0.05$, **$p < 0.01$ (Student's paired *t*-test).

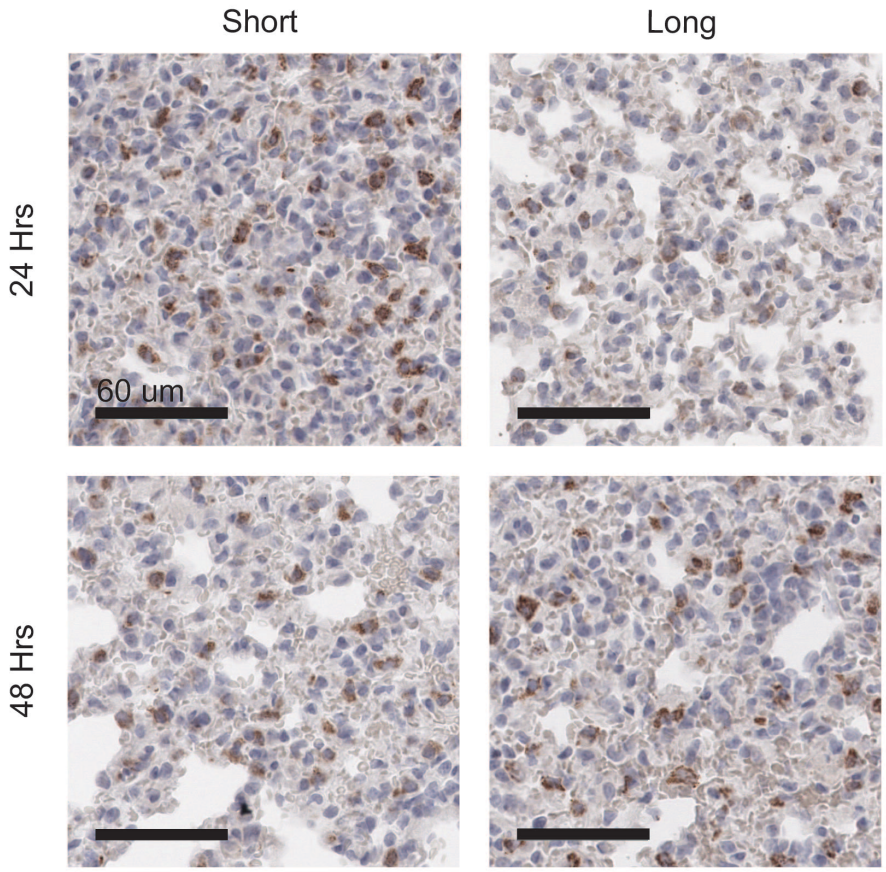

Figure 1—figure supplement 1: Long glycopolymers delay MCF-10A cell death in nude mice MCF-10A cells were painted with either short or long glycopolymers and injected into the tail veins of nude mice. At the time points indicated, the mice were sacrificed and their lungs fixed and paraffin embedded. Sections were stained by immunohistochemistry for the cell death marker cleaved caspase-3 (CC3) (brown). Nuclei are counterstained with hematoxylin. There is not only less CC3 expression 24 hours after injection in the long glycopolymer-bearing cells compared to the short, but also, whereas the short-treated cells experience the greatest death at 24 hours and subsequently signal decreases, the long glycopolymer-bearing cells don't peak in CC3 expression until 48 hours after injection. This delay in the timing of cell death implies a protective effect provided by the glycopolymers that is dependent upon size. Shown are micrographs representative of at least three biological replicates. Scale bars are 60 μm.

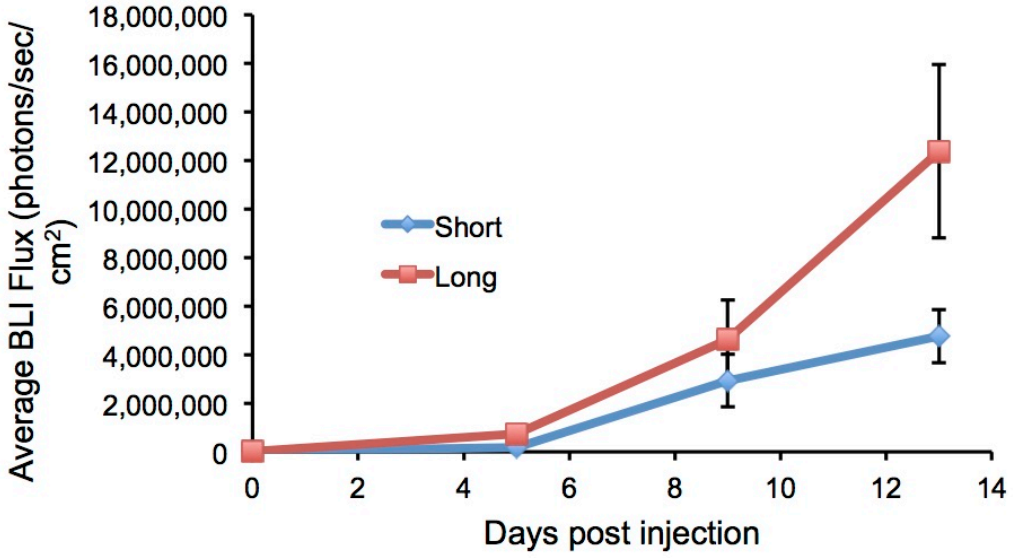

Figure 1—figure supplement 2: Long glycopolymer-bearing 4TO7 cells proliferate more rapidly in mouse lungs than those bearing short glycopolymers Animals were injected on day 0 with 4TO7 cells treated with either long or short cell-surface glycopolymers. At a given day post injection, mice were anesthetized, administered luciferin by intraperitoneal injection, then imaged using a live animal imaging system. Exogenously administered cells express luciferase and generate photons upon treatment with luciferin. Data shown are mean ± SEM. n = 5 for Long and n = 6 for Short.

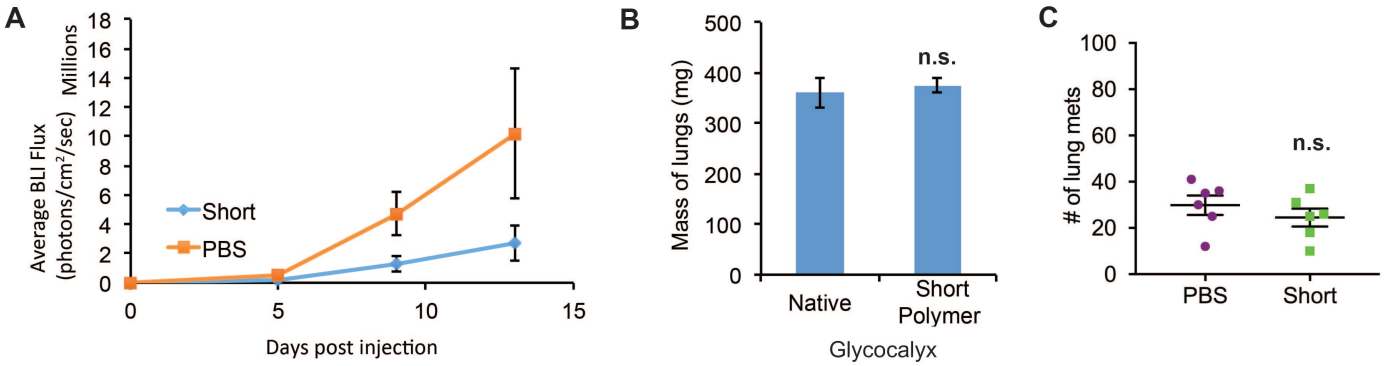

Figure 1—figure supplement 3: Short glycopolymer-bearing 4TO7 cells have no metastatic advantage over naïve 4TO7 cells Animals were injected on day 0 with cells treated with either short cell-surface glycopolymers or PBS vehicle. A) Quantification of bioluminescence imaging of anesthetized mice. At a given day post injection, mice were anesthetized, administered luciferin by intraperitoneal injection, then imaged using a live animal imaging system. Exogenously administered cells express luciferase and generate photons upon treatment with luciferin. B) Wet weight of mouse lungs excised during necropsy. C) Frank mets were counted on whole lung sections at 5 mm into sectioning for each mouse and grouped according to glycopolymer treatment type of injected cells. Data shown are mean ± SEM. n = 6 for PBS and n = 6 for Short.

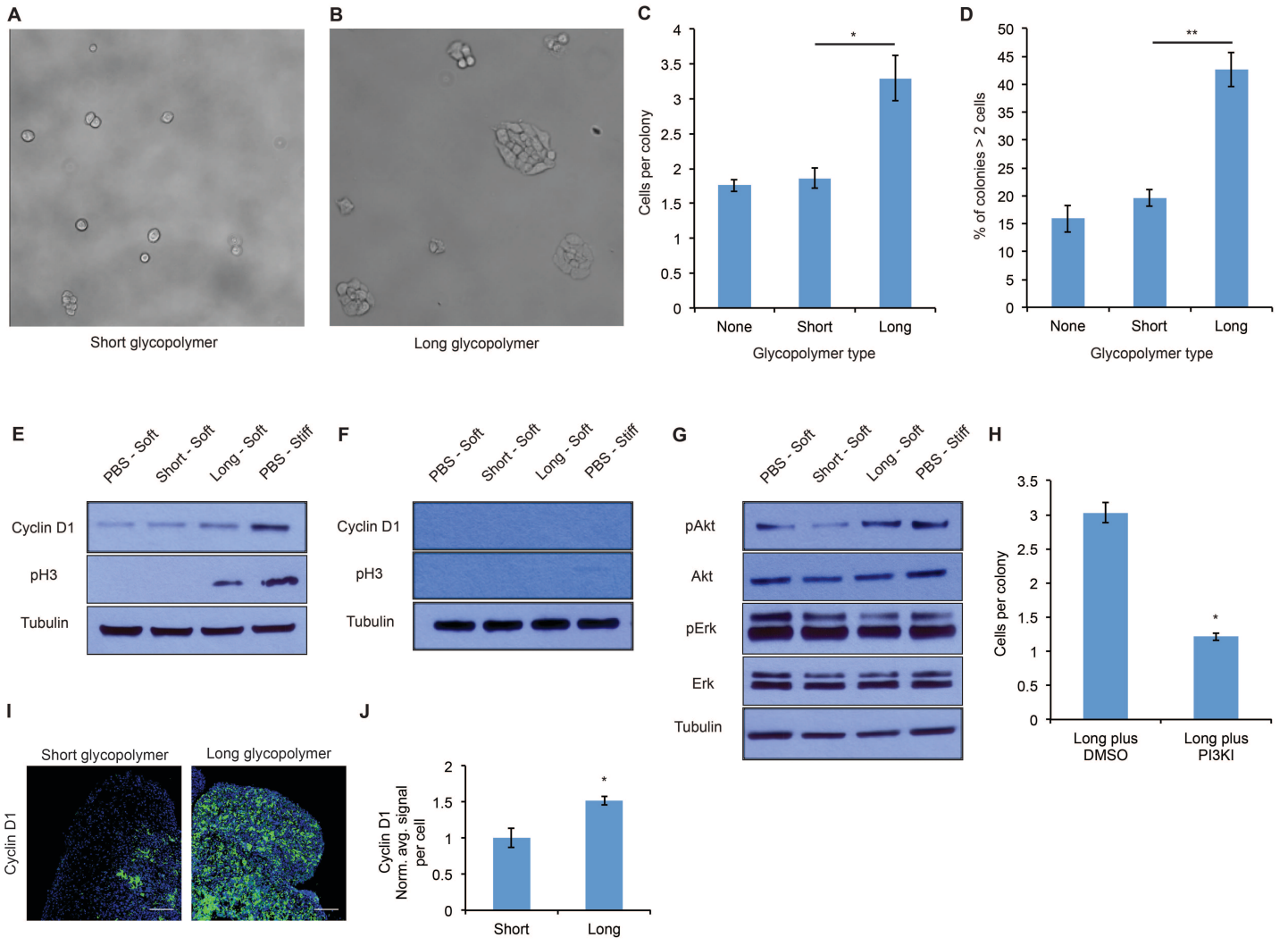

Figure 2: A thick glycocalyx drives cell cycle progression via the PI3K-Akt axis

A) and B) Microscopy of MCF-10A cells labeled with short or long glycopolymers, plated on soft (400 Pa) fibronectin-functionalized gels, and cultured for 72 hours. C) Average number of cells per colony in images such as B and C. D) Percent of colonies containing more than 2 cells in images such as B and C. E) Immunoblot analysis of proliferative markers in MCF-10A cells coated with long or short glycopolymers or treated with vehicle (PBS) and plated on soft (400 Pa) or stiff (60 kPa) fibronectin-functionalized polyacrylamide gels for six hours. F) Immunoblot of MCF-10A cells serum-starved for 72 hours, treated with long or short glycopolymers or vehicle and plated in serum-free media on soft or stiff gels for six hours. G) Immunoblot analysis of pAkt and pErk in serum-starved MCF-10A cells treated and plated as in F, allowed to adhere for six hours, then challenged with epidermal growth factor for 15 minutes, and lysed. H) Average number of cells per colony of long glycopolymer-bearing MCF-10A cells plated on soft gels in media containing 50 μM PI3K inhibitor LY294002 or vehicle (DMSO) and cultured for 72 hours. I) Cyclin D1 (green) IF staining of mets from experiments in Fig. 1. DAPI nuclear stain in blue. J) Quantification of IF staining normalized to the average

signal per nuceli in mets from short glycopolymer treated cells. Shown is mean ± SEM of three mice per group from which 3-4 tumors were averaged each. For C, D, and H, shown is the mean ± SEM of three biological replicate experiments. For E-G, blots are representative of experiments performed at least twice. Scale bars are 100 μm. *$p < 0.05$, **$p < 0.01$ (Student's paired *t*-test).

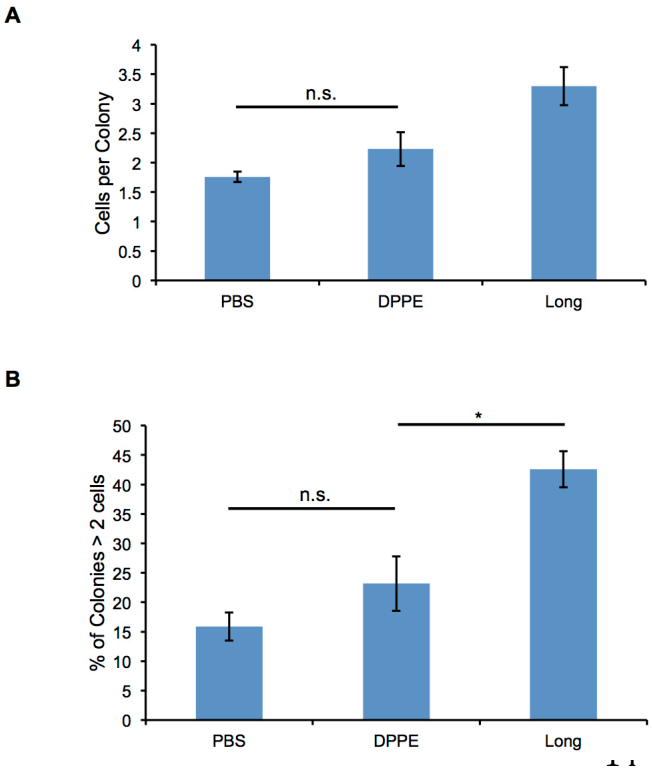

Figure 2—figure supplement 1: Glycopolymers must be cell-surface resident to affect colony size

A) Average number of cells per colony of MCF-10A cells treated with cell-surface persistent (Long) or rapidly endocytosed but equally long (DPPE) mucin-mimetic glycopolymers then plated at low density on soft (140 Pa) fibronectin-functionalized polyacrylamide gels. B) Percent of colonies containing more than two cells of cells treated as in A. Shown is mean ± SEM of three biological replicate experiments in which nine fields of view were imaged randomly from each of two technical replicate gels. n.s. - not significant. *$p < 0.05$. (Student's paired *t*-test).

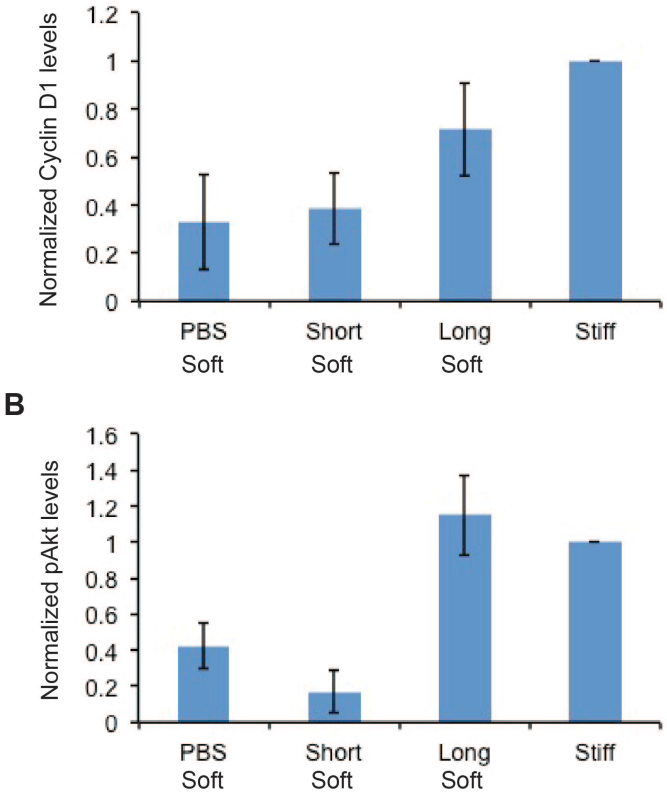

Figure 2—figure supplement 2: Quantification of western blots A) Western blots from Figure 2E were analyzed by densitometry, their values normalized first to total protein (tubulin) then to that of the positive control—PBS treated cells on a stiff Fn-functionalized matrix. B) Western blots from Figure 2G were quantified and normalized as in A. Shown are mean ± SEM of two replicate experiments.

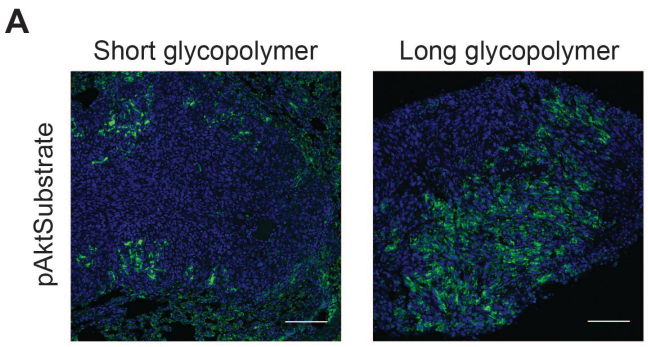

Figure 2—figure supplement 3: Long glycopolymers increase active Akt in 4TO7 lung metastases Tissue sections from lungs derived from the experiments described in figure 1 were stained with an anti-pAkt substrate antibody. The antibody is selective for a phosphorylated consensus sequence known to be targeted by pAkt and thereby gives an indirect measure of Akt activity. Shown are fluoromicrographs representative of at least three independent experiments.

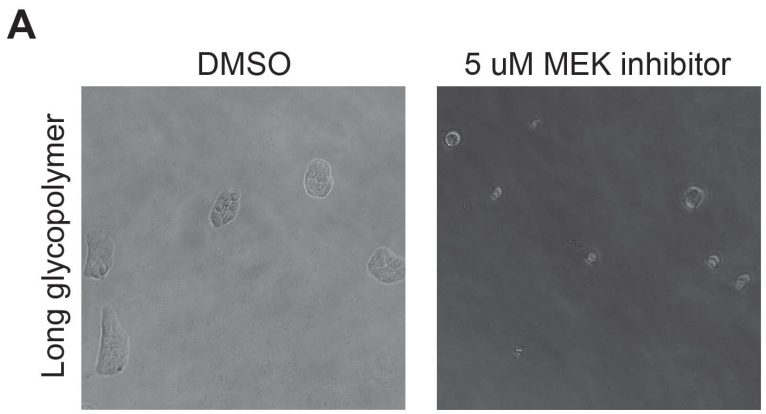

Figure 2—figure supplement 4: MEK inhibitor prevents effects of Long glycopolymers on proliferation

Long glycopolymer-bearing MCF-10A cells seeded on soft polyacrylamide gels functionalized with fibronectin in media supplemented with 5 μM of the specific MEK inhibitor U0126 or DMSO vehicle alone after 72 hours.

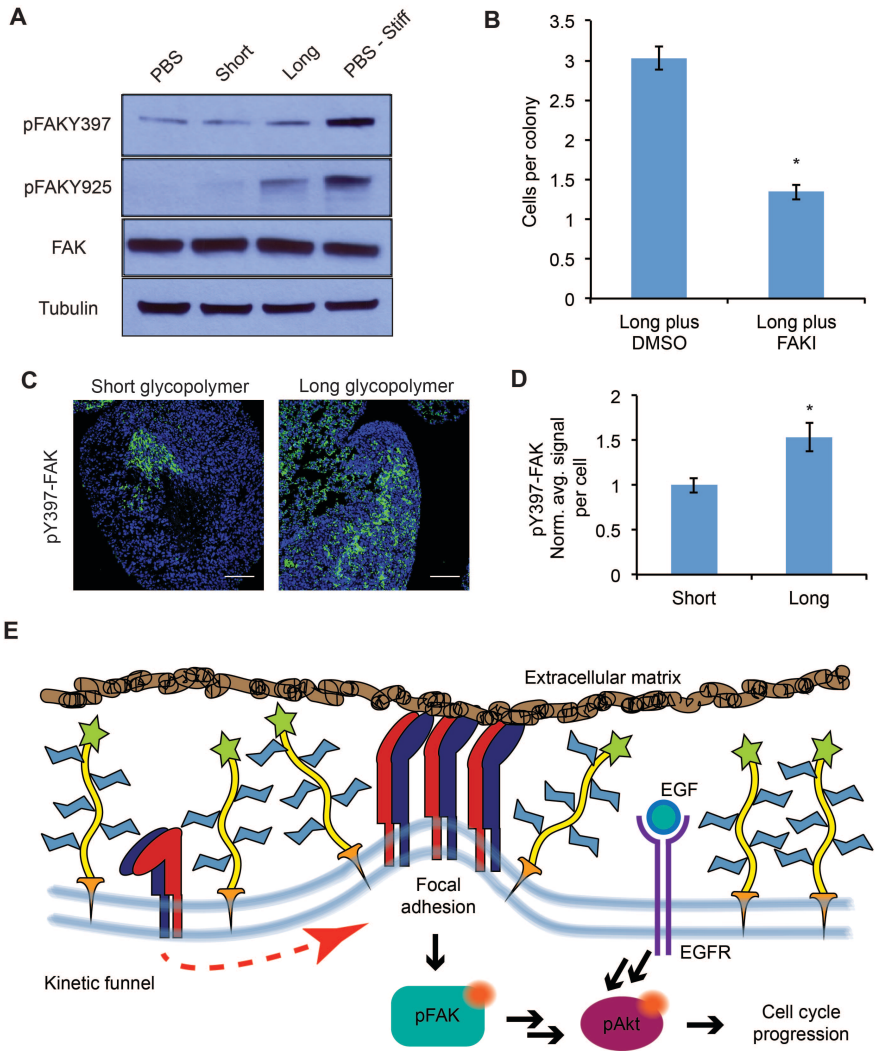

Figure 3: A thick glycocalyx stimulates integrin-FAK mechanosignaling

A) Immunoblot analysis of FAK phosphorylation in MCF-10A cells coated with long or short glycopolymers or treated with vehicle (PBS) and plated on soft (400 Pa) or stiff (60 kPa) fibronectin-functionalized polyacrylamide gels for six hours. B) Average number of cells per colony of long glycopolymer-bearing MCF-10A cells plated on soft gels in media containing 1 μM FAK inhibitor FAK14 or vehicle (DMSO) and cultured for 72 hours. C) pY397-FAK IF staining in green of mets from experiments in Fig. 1. DAPI nuclear stain in blue. D) Quantification of IF staining in C normalized to the average signal per nuceli in mets from short glycopolymer-treated cells. Shown is mean ± SEM of three mice per group from which 3-4 tumors were averaged each. E) A model by which a mucin-bolstered glycocalyx may drive proliferation. Limited ligand access due to steric hindrance establishes a kinetic funnel in which integrins are likely to bind where bonds exist already. This drives a clustering of integrins that activates FAK which, in conjunction with EGFR, drives activation of Akt and subsequently cell cycle progression. Blot in A is representative of at least three biological

replicate experiments. Shown in B is mean ± SEM from three biological replicate experiments. Scale bars are 100 μm. *$p < 0.05$ (Student's paired *t*-test).

A

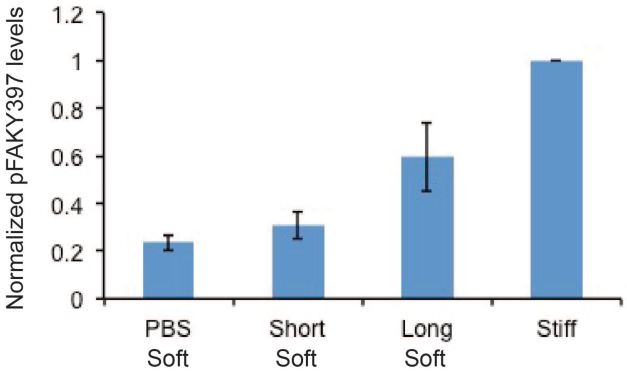

Figure 3—figure supplement 1: Quantification of western blots A) Western blots from Figure 3A were analyzed by densitometry, their values normalized first to total protein (tubulin) then to that of the positive control—PBS treated cells on a stiff fibronectin-functionalized matrix. Shown are mean ± SEM of three biological replicates.

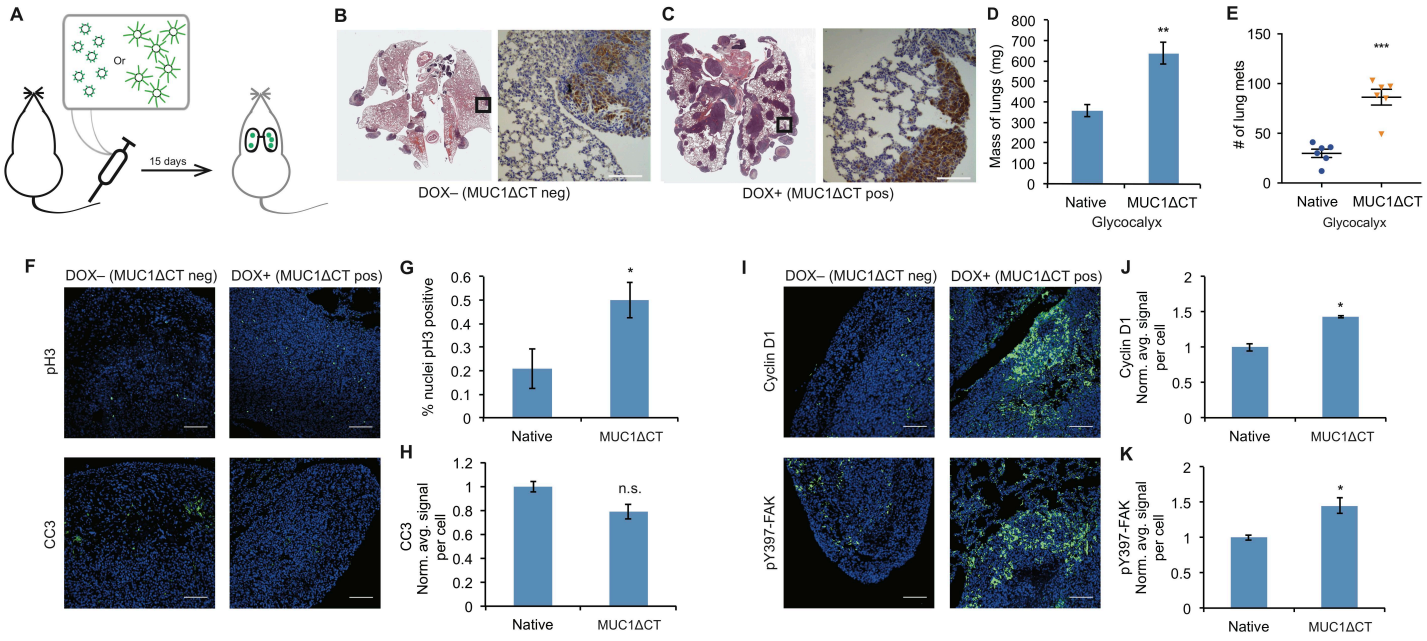

Figure 4: The MUC1 ectodomain is sufficient to increase the metastatic potential of 4TO7 cancer cells

A) Experimental scheme for Figure 4. Balb/c mice were injected with syngeneic 4TO7 mammary carcinoma cells transfected with a MUC1ΔCT construct under the control of a doxycycline (dox)-inducible promoter. Cells were treated with either dox 200 ng/ml or vehicle (PBS) for 24 hrs before injections. B) and C) Whole lung sections H&E stained and IHC labeled for mCherry indicating presence of exogenously introduced cells. D) Lungs excised during necropsy were weighed, wet, before fixing. E) Frank mets were counted on whole lung sections at 5 mm into sectioning for each mouse and grouped according to treatment type of injected cells. F) IF staining of mets for the mitotic marker pH3 or apoptotic marker CC3 in green. DAPI nuclear staining is shown in blue. G) and H) Quantification of IF signal. For pH3, shown is the quotient of positive over total nuclei. I) Cyclin D1 and pY397-FAK IF staining of mets in green. DAPI nuclear stain in blue. J) and K) Quantification of IF signal. For H, J, and K, total signal was normalized to the average signal per nuceli in mets from PBS treated cells. Shown is mean ± SEM of three mice per group from which 3-4 tumors were averaged each. For D and E, shown is the mean ± SEM of n = 6 for mice injected with PBS-treated cells and n = 6 for mice injected with dox-treated cells. Scale bars are 100 μm. *$p < 0.05$, **$p < 0.01$, ***p<0.001 (Student's paired *t*-test).

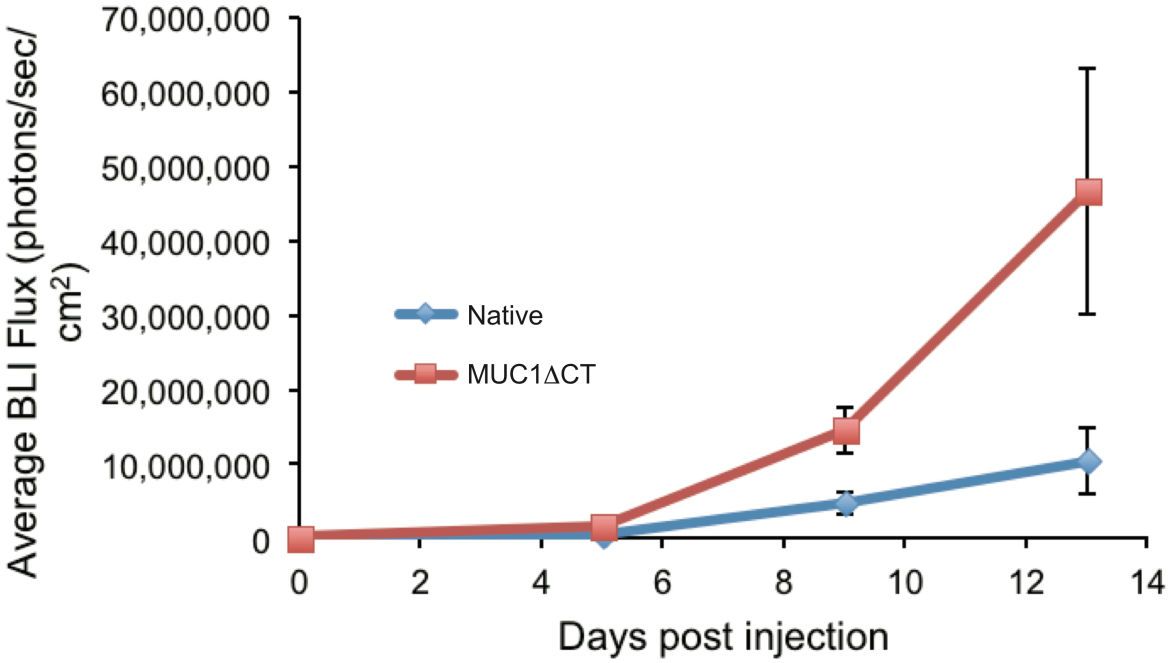

Figure 4—figure supplement 1: 4TO7 cells expressing the MUC1 ectodomain proliferate more rapidly in mouse lungs than those that do not Animals were injected on day 0 with 4TO7 cells treated with either doxycycline to induce expression of MUC1ΔCT construct or PBS vehicle (Native). At a given day post injection, mice were anesthetized, administered luciferin by intraperitoneal injection, then imaged using a live animal imaging system. Exogenously administered cells express luciferase and generate photons upon treatment with luciferin. Data shown are mean ± SEM of n = 6 for both groups.

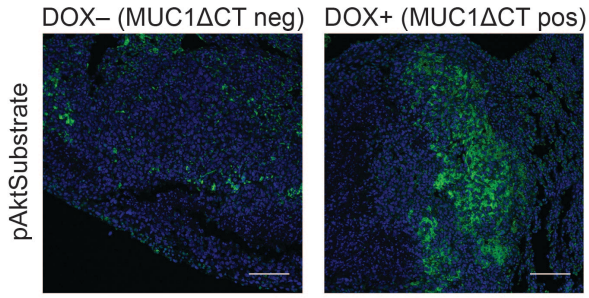

Figure 4—figure supplement 2: The MUC1 ectodomain increases Akt activity in 4TO7 lung metastases

Tissue sections from lungs derived from the experiments described in figure 4 were stained with an anti-pAkt substrate antibody. The antibody is selective for a phosphorylated consensus sequence known to be targeted by pAkt and thereby gives an indirect measure of Akt activity. Shown are fluoromicrographs representative of at least three independent experiments.

References

1. Bast RC, Hennessy B, Mills GB, Mills GB. The biology of ovarian cancer: new opportunities for translation. Nat Rev Cancer. 2009 Jun;9(6):415–28.
2. Rahn JJ, Dabbagh L, Pasdar M, Hugh JC. The importance of MUC1 cellular localization in patients with breast carcinoma: an immunohistologic study of 71 patients and review of the literature. Cancer. 2001 Jun 1;91(11):1973–82.
3. Kufe DW. Mucins in cancer: function, prognosis and therapy. Nat Rev Cancer. 2009;9(12):874–85.
4. Hattrup CL, Gendler SJ. Structure and Function of the Cell Surface (Tethered) Mucins. Annu Rev Physiol. 2008 Mar;70(1):431–57.
5. Paszek MJ, DuFort CC, Rossier O, Bainer R, Mouw JK, Godula K, Hudak JE, Lakins JN, Wijekoon AC, Cassereau L, Rubashkin MG, Magbanua MJ, Thorn KS, Davidson MW, Rugo HS, Park JW, Hammer D a., Giannone G, Bertozzi CR, Weaver VM. The cancer glycocalyx mechanically primes integrin-mediated growth and survival. Nature. 2014;511(7509):319–25.
6. Freeman SA, Goyette J, Furuya W, Woods EC, Bertozzi CR, Bergmeier W, Hinz B, van der Merwe PA, Das R, Grinstein S. Integrins Form an Expanding Diffusional Barrier that Coordinates Phagocytosis. Cell. 2016 Jan 14;164(1–2):128–40.
7. Paszek MJ, Boettiger D, Weaver VM, Hammer DA. Integrin clustering is driven by mechanical resistance from the glycocalyx and the substrate. PLoS Comput Biol. 2009;5(12).
8. Woods EC, Yee NA, Shen J, Bertozzi CR. Glycocalyx Engineering with a

Recycling Glycopolymer that Increases Cell Survival In Vivo. Angew Chemie Int Ed. 2015 Dec 21;54(52):15782–8.

9. Desgrosellier JS, Cheresh DA. Integrins in cancer: biological implications and therapeutic opportunities. Nat Rev Cancer. 2010 Jan;10(1):9–22.

10. Wang X, Lan H, Li J, Su Y, Xu L. Muc1 promotes migration and lung metastasis of melanoma cells. Am J Cancer Res. 2015;5(9):2590–604.

11. Spicer AP, Rowse GJ, Lidner TK, Gendler SJ. Delayed mammary tumor progression in Muc-1 null mice. J Biol Chem. 1995 Dec 15;270(50):30093–101.

12. Hudak JE, Canham SM, Bertozzi CR. Glycocalyx engineering reveals a Siglec-based mechanism for NK cell immunoevasion. Nat Chem Biol. 2014;10(1):69–75.

13. Godula K, Umbel ML, Rabuka D, Botyanszki Z, Bertozzi CR, Parthasarathy R. Control of the molecular orientation of membrane-anchored biomimetic glycopolymers. J Am Chem Soc. 2009;131(29):10263–8.

14. Eng ET, Smagghe BJ, Walz T, Springer TA. Intact ?? IIb?? 3 integrin is extended after activation as measured by solution x-ray scattering and electron microscopy. J Biol Chem. 2011;286(40):35218–26.

15. Miller FR, Soule HD, Tait L, Pauley RJ, Wolman SR, Dawson PJ, Heppner GH. Xenograft model of progressive human proliferative breast disease. J Natl Cancer Inst. 1993 Nov 3;85(21):1725–32.

16. Paszek MJ, Zahir N, Johnson KR, Lakins JN, Rozenberg GI, Gefen A, Reinhart-King CA, Margulies SS, Dembo M, Boettiger D, Hammer DA, Weaver VM. Tensional homeostasis and the malignant phenotype. Cancer Cell. 2005 Sep;8(3):241–54.

17. Aslakson CJ, Miller FR. Selective events in the metastatic process defined by analysis of the sequential dissemination of subpopulations of a mouse mammary tumor. Cancer Res. 1992 Mar 15;52(6):1399–405.

18. Chambers AF, Groom AC, MacDonald IC. Metastasis: Dissemination and growth of cancer cells in metastatic sites. Nat Rev Cancer. 2002 Aug;2(8):563–72.

19. Lakins JN, Chin AR, Weaver VM. Exploring the link between human embryonic stem cell organization and fate using tension-calibrated extracellular matrix functionalized polyacrylamide gels. Methods Mol Biol. 2012;916:317–50.

20. Discher DE, Janmey P, Wang Y. Tissue Cells Feel and Respond to the Stiffness of Their Substrate. Science (80-). 2005;310(5751).

21. Kuwada SK, Li X. Integrin alpha5/beta1 mediates fibronectin-dependent epithelial cell proliferation through epidermal growth factor receptor activation. Mol Biol Cell. 2000 Jul;11(7):2485–96.

22. Moreno-Layseca P, Streuli CH. Signalling pathways linking integrins with cell cycle progression. Matrix Biol. 2014;34:144–53.

23. Mitra SK, Hanson DA, Schlaepfer DD. Focal adhesion kinase: in command and control of cell motility. Nat Rev Mol Cell Biol. 2005 Jan;6(1):56–68.

24. Kufe DW. Functional targeting of the MUC1 oncogene in human cancers. Cancer Biol Ther. 2009 Jul;8(13):1197–203.

25. Cox AD, Fesik SW, Kimmelman AC, Luo J, Der CJ. Drugging the undruggable RAS: Mission Possible? Nat Rev Drug Discov. 2014 Oct 17;13(11):828–51.

26. Horm TM, Schroeder JA. MUC1 and metastatic cancer: expression, function and therapeutic targeting. Cell Adh Migr. 2013;7(2):187–98.

27. Duffy MJ, Shering S, Sherry F, McDermott E, O'Higgins N. CA 15-3: a prognostic marker in breast cancer. Int J Biol Markers. 15(4):330–3.

28. Retterspitz MF, Mönig SP, Schreckenberg S, Schneider PM, Hölscher AH, Dienes HP, Baldus SE. Expression of {beta}-catenin, MUC1 and c-met in diffuse-type gastric carcinomas: correlations with tumour progression and prognosis. Anticancer Res. 2010 Nov;30(11):4635–41.

29. McGuckin MA, Walsh MD, Hohn BG, Ward BG, Wright RG. Prognostic significance of MUC1 epithelial mucin expression in breast cancer. Hum Pathol. 1995 Apr;26(4):432–9.

30. Belisle JA, Horibata S, Gubbels JAA, Petrie S, Kapur A, Andre S, Gabius H-J, Rancourt C, Connor J, Paulson JC, Patankar MS. Identification of Siglec-9 as the receptor for MUC16 on human NK cells, B cells, and monocytes. Mol Cancer. 2010;9(1):118.

31. Ohta M, Ishida A, Toda M, Akita K, Inoue M, Yamashita K, Watanabe M, Murata T, Usui T, Nakada H. Immunomodulation of monocyte-derived dendritic cells through ligation of tumor-produced mucins to Siglec-9. Vol. 402, Biochemical and Biophysical Research Communications. 2010.

32. Beatson R, Tajadura-Ortega V, Achkova D, Picco G, Tsourouktsoglou T-D, Klausing S, Hillier M, Maher J, Noll T, Crocker PR, Taylor-Papadimitriou J, Burchell JM. The mucin MUC1 modulates the tumor immunological microenvironment through engagement of the lectin Siglec-9. Nat Immunol. 2016 Sep 5;

33. Yang J, Mani SA, Donaher JL, Ramaswamy S, Itzykson RA, Come C, Savagner P,

1 Gitelman I, Richardson A, Weinberg RA. Twist, a Master Regulator of
2 Morphogenesis, Plays an Essential Role in Tumor Metastasis. Cell.
3 2004;117(7):927–39.
4